Chemical Engineering Journal 143 (2008) 282–292

Contents lists available at ScienceDirect

Chemical Engineering Journal

journal homepage: www.elsevier.com/locate/cej

Nonlinear predictive control of a polymerization reactor based on piecewise linear Wiener model

G. Shafiee, M.M. Arefi*, M.R. Jahed-Motlagh, A.A. Jalali

Iran University of Science and Technology, Tehran 16846, Iran

ARTICLE INFO

Article history:
Received 18 February 2008
Received in revised form 23 April 2008
Accepted 5 May 2008

Keywords:
Nonlinear model predictive control (NMPC)
Piecewise linear (PWL) Wiener model
Generalized multiple-level noise (GMN)
Quadratic programming (QP)
Polymerization reactor
Multi-input multi-output (MIMO)

ABSTRACT

In this paper, a nonlinear model predictive control (NMPC) based on a piecewise linear Wiener model is applied to a polymerization reactor. The static nonlinear part of the applied Wiener model is approximated using the piecewise linear functions and its dynamic linear element is identified using a state-space description. Due to the nonlinear gain of model, for gathering data, a generalized multiple-level noise (GMN) test has been used. This test demonstrates the response of the system to a range of amplitude changes. The predictive control based on this model retains all the interested properties of the classical linear MPC. This approach leads to a quadratic programming problem due to the canonical structure of the nonlinear gain. The control scheme has been applied to a polymerization reactor as a MIMO process. Results show that the used Wiener model is able to identify the nonlinear processes effectively. The nonlinear predictive control based on this model is compared to the linear MPC. The parameters of both linear and nonlinear model predictive controllers are tuned and the performances of both methods are compared. It is shown that the nonlinear controller has a better performance, having short settling time and without any overshoot compared to its linear one. Moreover, this controller has a good performance and rejects unmeasured disturbances effectively.

1. Introduction

There are very few design techniques that can be proven to stabilize processes in the presence of nonlinearities and constraints. Model predictive control (MPC) is one of these techniques [1]. MPC refers to a class of computer control algorithms that control the future behavior of a plant through the use of an explicit process model. At each control interval the MPC algorithm computes an open-loop sequence of manipulated variable adjustments in order to optimize future plant behavior. The first input in the optimal sequence is injected into the plant, and the entire optimization is repeated at subsequent control intervals [1]. Regarding desirable properties of MPC, these controllers are applied quickly in a wide range of different industries; such that by the year 1999 more than 4500 applications of these controllers have been reported which use linear model, while about 80% of these applications are in petrochemical industries [2,3]. By now, the application of MPC based on linear dynamic models covers a wide range of applications and the linear MPC theory can be considered quite mature [1]. Nevertheless, many manufacturing processes are inherently nonlinear and there are cases where nonlinear effects are significant and can not be ignored. These include at least two broad categories of applications [1]:

1- Regulator control problems where the process is highly nonlinear and subject to large frequent disturbances (pH control, etc.).
2- Servo control problems where the operating points change frequently and span a wide range of nonlinear process dynamics (polymer manufacturing, ammonia synthesis, etc.).

Under these conditions, linear models are often not sufficient enough to describe the process dynamics adequately and therefore nonlinear models should be used. Nonlinear model predictive control (NMPC) is a good development of linear MPC to nonlinear world that is presented as a very good scheme for this type of problems. NMPC is conceptually similar to its linear counterpart except that nonlinear dynamic models are used for process prediction and optimization [4].

Nonlinear systems modeling can be performed in three different ways. The first method is the use of different models for various operating points of the system. The second approach is using fundamental equations (e.g. mass and energy conservation equations) which in most cases are difficult to use due to process complexity.

* Corresponding author. Tel.: +98 21 77240492; fax: +98 21 77240490.
E-mail address: arefi@iust.ac.ir (M.M. Arefi).

1385-8947/$ – see front matter © 2008 Elsevier B.V. All rights reserved.
doi:10.1016/j.cej.2008.05.013

Nomenclature

A_c	heat-transfer area of the reactor
c_p	specific heat capacity of reactor contents
D	polydispersity
Da_j	Damkohler number for species j
E_j	activation energy for reaction j
f	initiator efficiency
g_t	gel effect factor
h	heat-transfer coefficient
$-\Delta H$	heat of reaction
I	initiator concentration in the reactor
I_f	initiator feed concentration
k_d	dissociation rate constant for initiator
k_f	rate constant for chain transfer to monomer
k_{fs}	rate constant for chain transfer to solvent
k'_i	frequency factor for reaction i ($i = d, f, p, t$)
k_p	propagation rate constant
k_t	overall termination rate constant
k_{tc}	rate constant for combination termination
k'_{tco}	zero conversion frequency factor for combination termination reaction
k_{td}	rate constant for disproportionation
k'_{tdo}	zero conversion frequency factor for disproportionation reaction
k_{to}	overall termination rate constant at zero conversion
k'_{to}	frequency factor for overall termination rate constant at zero conversion
M	monomer concentration in the reactor
M_f	monomer feed concentration
M_{fo}	monomer feed concentration for scaling purposes only
MW_i	molecular weight for initiator
MW_m	molecular weight for monomer
MW_s	molecular weight for solvent
P	concentration of live polymer
q	volumetric flow rate
R	universal gas constant
S	solvent concentration
t	time
T, T_c	reactor temperature, jacket temperature
T_f	feed temperature
u	vector of manipulated variables
v_k	white noise sequence, measurement
V	volume of reactor
V_f	free volume
V_{fm}, V_{fp}, V_{fs}	free volume contribution of monomer, polymer, solvent, respectively
V_{if}	volume fraction of initiator in feed
V_{mf}	volume fraction of monomer in feed
w	white noise input, process
W	dimensionless live polymer concentration
x_i	dimensionless reactor state variable
x_{1f}	manipulated variable (dimensionless inlet monomer concentration)
x_{2c}	manipulated variable (dimensionless jacket temperature)
x_{3f}	manipulated variable (dimensionless inlet initiator concentration)

Greek letters

β	dimensionless heat-transfer coefficient
ϕ_m, ϕ_p, ϕ_s	volume fraction of monomer, polymer, solvent, respectively
λ_0, λ_1, λ_2	zeroth, first, and second MWD moments
μ	number-average chain length
ρ	density of reacting medium
ρ_s, ρ_i, ρ_m	densities of solvent, initiator, and monomer, respectively
τ	dimensionless time

Subscripts

D, f	dissociation, transfer to monomer
p	propagation
t_c, t_d	termination: combination, disproportionation
1, 2, 3, 4	monomer, temperature, initiator, solvent
5, 6, 7	moments: zeroth, first, second

The third and the best approach is the use of empirical models that convert the available input–output data to an input–output relation which can be used for the prediction of the future behavior of the system.

There are several approaches to nonlinear system identification based on empirical models. One way is to use theoretically sound nonlinear functions and to develop identification schemes for these models. Identification using Volterra series, neural networks and nonlinear ARMAX models belong to this methodology. The advantage of this approach is the ability to obtain a global model of the underlying system. The main difficulty of the approach is the high cost in identification tests and computation. Another approach is to combine linear dynamic models with static or memoryless nonlinear functions. These types of models are called *block-oriented nonlinear models*. There are several advantages when using block-oriented models: (1) low cost in identification tests; (2) low cost in identification and control computations and (3) it is easy to comprehend and to incorporate *a priori* process knowledge [5].

The class of block-oriented nonlinear models includes complex models which are composed of linear dynamic systems and nonlinear static elements. Wiener and Hammerstein models are the most known and the most widely implemented members of this class. Wiener and Hammerstein models have found numerous industrial applications for system modeling, control, fault detection and isolation. Wiener and Hammerstein models reveal the capability of describing a wide class of different systems and apart from industrial examples, there are many other applications in biology and medicine [6].

In particular, Wiener models have a special structure that facilitates their application to NMPC. These models consist of a linear dynamic element which is followed by a static nonlinearity and can represent many of the nonlinearities commonly encountered in industrial processes [7]. Due to the static nature of the nonlinearities, they can be removed from the control problem. This fact generalizes the well-known gain-scheduling concept for nonlinear control. Due to the presence of some potential computational difficulties, an implicit inversion of the nonlinear static gain is necessary [7]. Application of these models in NMPC has been addressed in several papers [7–15]. For example in Refs. [8,9], a static nonlinear term is used to model the inverse of the nonlinearity of the plant and is selected as a polynomial with proper degree. Besides in Refs. [7,10,11], the nonlinear term and its inverse are modeled using piecewise linear (PWL) method. In Ref. [12], a nonlinear combination of Laguerre models followed by a single-layer neural network is introduced as an efficient nonlinear identification method used in MPC applications. The nonlinear predictive control based on Wiener-Neural model is presented in Ref. [13], where the static nonlinear part is modeled using neural network. In all of these works the paradigmatic applications have been pH neutralization and continuous stirred tank reactor (CSTR) processes. In Ref. [14], the nonlinear predictive control based on a Wiener-Neural model is applied to a plug-flow tubular reactor, where the process is simulated in HYSYS environment. In Ref. [15], a distillation column simulation model is used as a benchmark to demonstrate the benefits of a Wiener model based identification and control methodology. The results verify the capability of this method in identification of a nonlinear ill-conditioned plant compared with the other existing linear techniques.

In addition to the above-mentioned processes, a polymerization reactor is a process that bears a highly nonlinear behavior. Polymerization reactors are difficult to control effectively due to their highly nonlinear behavior and multi-input multi-output structure.

Lack of online measurements and input constraints are two important problems which are sometimes neglected in academic studies of a polymerization reactor control [16,17]. Most nonlinear control techniques proposed for polymerization reactors are based on feedback linearization or MPC [17–21]. In Ref. [17], a multivariable extension of the feedback linearization (FBL) MPC control strategy for the free-radical polymerization of methyl methacrylate in a CSTR has been presented and its results are compared to NMPC. A constrained MPC of a polymerization reactor is presented in Ref. [18], where the process is controlled as three inputs–three outputs. In Ref. [19], a multi-input multi-output (MIMO) Wiener model of a polymerization reactor is identified and the model is used in an MPC scheme. The quality of the proposed controller is also compared with that of linear MPC. This algorithm is based on the past inputs multivariable output error state-space (PI-MOESP) method for the estimation of system matrices of the linear part [22], and Tchebychev polynomials for the nonlinear part [19]. In Ref. [20], an adaptive MPC is applied to methyl methacrylate (MMA) polymerization reactor. The control of a solution copolymerization reactor using MPC algorithm based on multiple piecewise linear models is presented in Ref. [21].

In this paper, a nonlinear model predictive control based on a piecewise linear Wiener model is applied to a polymerization reactor. The static nonlinear element of this Wiener model is approximated using the piecewise linear functions and its dynamic linear element is modeled using a state-space description. PWL functions have been proved to be a very powerful tool for modeling and analyzing nonlinear systems [23,24]. A generalized multiple-level noise (GMN) test [5] is used for getting data in order to identify the model. The presented control scheme has been applied to a polymerization reactor, and its results have been compared to linear MPC.

The paper is organized as follows: In Section 2 a Wiener model with a piecewise linear representation for the nonlinear gain is presented and then the NMPC based on this Wiener model is described. In Section 3, the presented control scheme has been applied to a polymerization reactor, and simulation results are compared to linear MPC. Finally, some concluding remarks are discussed in Section 4.

2. The nonlinear model predictive control based on piecewise linear Wiener model

In this section, nonlinear predictive control based on a piecewise linear Wiener model is introduced. For identification of this model, an efficient test signal for gathering dynamic data is necessary. To do this, some test signals are presented. By using obtained data, the procedure of the Wiener model identification and inverse model evaluation is stated. Finally, the NMPC based on this Wiener model is presented.

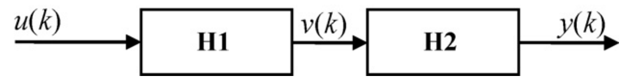

Fig. 1. The Wiener model.

2.1. Piecewise linear Wiener model

Among the nonlinear black box models, the block-oriented models are efficient structures in nonlinear modeling [14]. These models consist of a series connection of a linear dynamic and static nonlinear element.

A Wiener model consists of a dynamic linear block (**H1**) in cascade with a static nonlinearity at the output (**H2**), as shown in Fig. 1. Here $v(k) \in R^{m_o}$ is an intermediate signal that does not necessarily have a physical meaning. On the other hand, in the Hammerstein model the static input nonlinearity precedes the linear block.

In certain respects, Hammerstein models are very similar to the linear models on which they are based. For example, if $u(k)$ is a piecewise constant input sequence [e.g. pulses, steps, pseudo-random binary sequences (PRBS), etc.], for any static nonlinearity the intermediate variable sequence will also be a piecewise constant sequence with the same general character (specifically, with transitions at the same instants as $u(k)$, but assuming different values). Hammerstein models have been considered as alternatives to linear models in a number of chemical process applications [25].

In particular, while Hammerstein and Wiener models exhibit exactly the same steady-state behavior, the differences in their transient responses can be quite significant. As a specific example, the general character of the step response can change with the sign and/or magnitude of the input step, unlike the case of the Hammerstein model, where this general character is determined entirely by the linear part [25]. Because of this behavior and the capability of modeling complex nonlinear dynamics by Wiener models led us to the selection of this model structure. In this paper, the possibilities and the advantages of the use of a specific Wiener approximation to represent the model of the process are analyzed.

Let us assume that the system to be controlled can be described by the following discrete-time, nonlinear, state-space model [7,11]:

$$x(k+1) = f(x(k), u(k)) \tag{1}$$

$$y(k) = g(x(k)) + d(k)) \tag{2}$$

where $f : R^n \times R^{m_i} \to R^n$ and $g : R^n \to \times R^{m_o}$ are twice continuously differentiable functions, $x \in R^n$ is a vector of n state variables, $u \in R^{m_i}$ is a vector of m_i process inputs or manipulated variables, $d \in R^{m_o}$ is a vector of m_o additive disturbance variables, $y \in R^{m_o}$ is a vector of m_o process outputs and k is the sample time.

There are several options to describe the linear dynamic block in Wiener models. For example, some of the used representations include convolution models (step or impulse responses), autoregressive moving average with exogenous input (ARMAX) models, autoregressive with exogenous input (ARX) models, state-space models, etc. [9]. In this work, a state-space model is used as follows:

$$\begin{aligned} x(k+1) &= \mathbf{A}x(k) + \mathbf{B}u(k) \\ v(k) &= \mathbf{C}x(k) + \mathbf{D}u(k) \end{aligned} \tag{3}$$

where **A**, **B**, **C**, **D** are the system matrices with proper dimensions.

For the static nonlinear element (**H2**), the continuous PWL functions are used. PWL functions have been proved to be a very powerful tool for modeling and analyzing nonlinear systems [24].

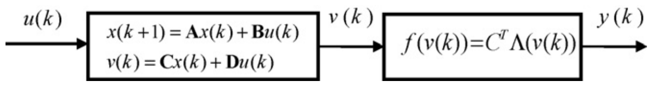

Fig. 2. The piecewise linear Wiener model.

It can be proved that any nonlinear function f ($f : R^{m_o} \to R^{m_o}$), can uniquely be represented as [24]:

$$f(v) = C^{\mathrm{T}}\Lambda(v) \tag{4}$$

where the vector $\Lambda = [\Lambda^{0\mathrm{T}}, \Lambda^{1\mathrm{T}}, \ldots, \Lambda^{m_o\mathrm{T}}]^{\mathrm{T}}$ is the elements of the basis and $C = [C_0^{\mathrm{T}}, C_1^{\mathrm{T}}, \ldots, C_{m_o}^{\mathrm{T}}]^{\mathrm{T}}$ is the parameter vector associated with the vector function Λ^i.

In this work, the function is $f = H_2 : D \to D$, being $D \in R^{m_o}$, as shown in Fig. 2. The domain and the image of the PWL function share the same dimension in our application. Moreover, if we assume that the function f of the system is invertible (this is a reasonable assumption for a large set of process models), it is possible to define the inverse function as f^{-1}, such that $v = f^{-1}(f(v))$. This function is also unique and PWL [10].

2.2. Input signal design

Some important factors which must be considered in designing the identification test for nonlinear systems are [5]:

a) Duration of the test signal.
b) Amplitude and shape of the test signal.
c) The spectrum of the test signal (the average switching time).
d) Correlation of the test signal in each channel.
e) The number of manipulated variables in each test.

Traditionally, PRBS are used as the inputs to a system in order to produce representative sets of data to be analyzed. In theory, a PRBS excites the range of dynamics present in a system so that a dynamic model can be produced which contains these dynamics. This is not sufficient, however, for fitting a Wiener model. Since these models have nonlinear gains, an input signal must be used which also demonstrates the response of the system to a range of amplitude changes [9]. A signal that satisfies these criteria is a GMN [5] or a modified PRBS signal [9] which, in addition to random frequency, also exhibits random amplitude changes.

In addition to above, one disadvantage of using a PRBS signal is that its spectrum has dips around some frequencies, which will result in low signal-to-noise ratios in these frequency ranges. A better way to generate binary signals with low-pass character is the so-called generalized binary sequence (GBN) [5]. Another advantage with GBN is that the signal length is flexible. The GBN also has a minimum crest factor [5].

Since in nonlinear systems the test time depends mainly on the number of parameters in the model and the level of noise and unmeasured disturbances, it is recommended longer test time in comparison with linear systems [5]. This is typically considered about 16–25 times of the settling time of the process. The other factors may be included by choosing one of the following test signals [5]:

a) Stair Test.
b) Filtered white uniform noise.
c) GMN.

In this work, the GMN test has been used for data collection. This type of test is a multi-level extension of GBN. In this test the amplitude and the number of pulses must be selected suitably. The number of levels on this test is equal or greater than the degree of the nonlinear polynomial which must be identified. Moreover, the average switching time of the test can be obtained from $T_{\mathrm{sw}} = T/3$, where T is 98% of the process settling time.

2.3. Wiener model identification and inverse model evaluation

Different Wiener model identification approaches can be found in relevant literature [7–15,19,22,26]. A general classification of these approaches is the following:

1) The N-L approach.
2) The L-N approach.
3) The simultaneous approach.

In this paper, the L-N approach is used for identification of Wiener model, because it is straightforward and ensures an accurate description of the static nonlinearity. In this method, first the linear block is identified using a correlation technique. After that, the intermediate signal v is generated from the input signal and finally the static nonlinearity is estimated.

For identification of Wiener model parameters, the linear part is modeled using a state-space description and the nonlinear static gain is identified using dynamic and steady-state input–output data. To identify the linear dynamic part and the static PWL function, the N4SID (Numerical Algorithms for Subspace State Space System Identification) algorithm and the PWL Toolbox [27] based on the least square method were used, respectively.

In order to implement the NMPC scheme that is described in the next section, a good representation of the inverse of the nonlinearity is necessary. To identify it, the following approaches are available [7,28]:

a) Algorithmic approach.
b) Direct inverse computation.
c) Direct identification.

Since problems of small dimension are dealt with here and useful data for the identification process are available, the direct identification approach has been chosen in this paper. In this method, after identification of linear model, the output sequences of this LTI system will be computed. With this sequence, a primary identification of the nonlinear part of the Wiener model can be estimated. Now, for identification of inverse of nonlinearity, the inputs and outputs of this sequence are changed and using this new sequence, the inverse of nonlinear element is identified for control purposes.

2.4. Nonlinear model predictive control

The control problem to be solved is to compute a sequence of inputs $\Delta u(k)$, $\{k = 1, \ldots, M\}$, that will minimize the following dynamic objective:

$$J = \sum_{j=1}^{P} ||y(k+j) - r||_{Q_j} + \sum_{j=0}^{M-1} ||\Delta u(k+j)||_{R_j} \tag{5}$$

subject to model equations and to inequality constraints:

$$\begin{aligned} y_l \le y(k+j) \le y_u \quad \forall j = 1, \ldots, P-1 \\ u_l \le u(k+j) \le u_u \quad \forall j = 1, \ldots, M-1 \end{aligned} \tag{6}$$

where P is the prediction horizon, M is the control horizon, u is the manipulated variable, y is the output variable and r is the desired set point. The relative importance of the objective function contributions is controlled by setting the time dependent weighting matrices Q_j and R_j. Beyond the control horizon, the control signal is assumed to be constant ($\Delta u(k+j)=0, j=M,\ldots,P$). Once $\Delta u(k)$ is computed, following the receding horizon principle, only the first element of the optimal control sequence is used as the current control value. Then the horizon will shift one step forward in time and the whole procedure is repeated.

In this work, since the PWL function f is assumed to be invertible; the inverse of nonlinear part of the Wiener model is used to translate set points, output variables and their constraints to the linear model. Finally, the Wiener NMPC (WNMPC) can be posed as a quadratic programming (QP) problem:

$$\begin{aligned}&\min_{\mathbf{u}(k)} J = \min_{\mathbf{u}(k)}\{(\hat{\mathbf{v}}(k)-\mathbf{r}^*(k))^{\mathrm{T}}\mathbf{Q}(\hat{\mathbf{v}}(k)-\mathbf{r}^*(k))+\mathbf{u}(k)^{\mathrm{T}}\mathbf{R}\,\mathbf{u}(k)\}\\ &\text{subject to}\\ &v_l \le \hat{v}(k) \le v_u\\ &u_l \le u(k) \le u_u\end{aligned} \tag{7}$$

where $\hat{\mathbf{v}}(k)$ is the predicted output for the linear model, $\mathbf{u}(k)$ is the vector of manipulating variables and $\mathbf{r}^*(k)=f^{-1}(\mathbf{r}(k))$ is a transformation of the set point $r(k)$ to the linear part. Also, the relative importance of the objective function contributions is controlled by setting the weighting matrices $\mathbf{Q}$ and $\mathbf{R}$.

3. Case study: polymerization rector

In this section, the presented control scheme is applied to a polymerization reactor as a MIMO process. Polymerization reactors are difficult to control effectively due to their highly nonlinear behavior and MIMO structure [17]. In this section, identification and predictive control of this process is presented.

3.1. Process description

The process under consideration is solution polymerization of methyl methacrylate (PMMA) in a jacketed CSTR. As shown in Fig. 3, three streams—monomer, initiator and solvent are feed into the CSTR system. The reactor is equipped with a cooling jacket to remove extra heat generated during the exothermic polymerization. The exit stream contains polymer product, unreacted polymer, initiator and solvent, and is send downstream for separation [18].

The model equations are [16]:

$$\dot{M} = \frac{q}{V}(M_{\mathrm{f}}-M) = k_{\mathrm{p}}MP \tag{8}$$

$$\dot{T} = \frac{q}{V}(T_{\mathrm{f}}-T)+\left(\frac{-\Delta H}{\rho c_{\mathrm{p}}}\right)k_{\mathrm{p}}MP-\frac{hA_{\mathrm{c}}}{V\rho c_{\mathrm{p}}}(T-T_{\mathrm{c}}) \tag{9}$$

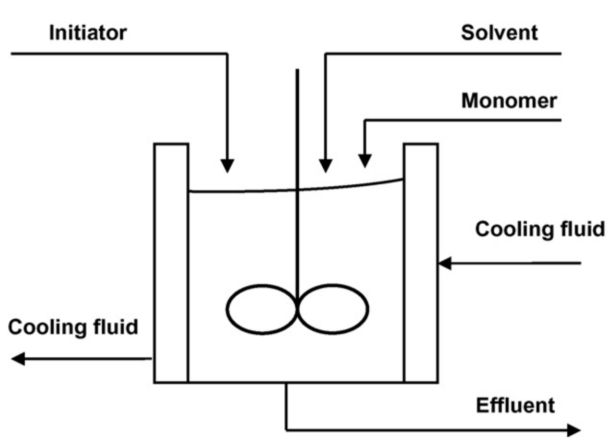

Fig. 3. Schematic of solution polymerization of MMA in a CSTR [18].

$$\dot{I} = \frac{q}{V}(I_{\mathrm{f}}-I)-k_{\mathrm{d}}I \tag{10}$$

$$\dot{S} = \frac{q}{V}(S_{\mathrm{f}}-S) \tag{11}$$

$$\dot{\lambda}_0 = -\frac{q}{V}\lambda_0+[(k_{\mathrm{f}}M+k_{\mathrm{td}}P+k_{\mathrm{fs}}S)]\alpha P+\frac{1}{2}k_{\mathrm{tc}}P^2 \tag{12}$$

$$\dot{\lambda}_1 = -\frac{q}{V}\lambda_1+\frac{[(k_{\mathrm{f}}M+k_{\mathrm{td}}P+k_{\mathrm{fs}}S)(2\alpha-\alpha^2)+k_{\mathrm{tc}}P]P}{(1-\alpha)} \tag{13}$$

$$\dot{\lambda}_2 = -\frac{q}{V}\lambda_2+\frac{[(k_{\mathrm{f}}M+k_{\mathrm{td}}P+k_{\mathrm{fs}}S)(\alpha^3-3\alpha^2+4\alpha)+k_{\mathrm{tc}}P(\alpha+2)]P}{(1-\alpha)^2} \tag{14}$$

where

$$\alpha = \frac{k_{\mathrm{p}}M}{k_{\mathrm{p}}M+k_{\mathrm{f}}M+k_{\mathrm{fs}}S+k_{\mathrm{t}}P} \tag{15}$$

$$P = \sqrt{\frac{2fk_{\mathrm{d}}I}{k_{\mathrm{I}}}} \tag{16}$$

$$k_{\mathrm{t}} = k_{\mathrm{tc}}+k_{\mathrm{td}} \tag{17}$$

The ith moment of the dead polymer molecular weight distribution (MWD) is represented by λ_i ($i=0$, 1, 2) and M is the monomer concentration, T is the reactor temperature, I is the initiator concentration, S is the solvent concentration, M_{f} is the monomer feed concentration, T_{f} is the feed temperature, I_{f} is the initiator feed concentration, S_{f} is the solvent feed concentration and T_{c} is the coolant temperature. Other process parameters are defined in notation part. The rate constants with the exception of k_{fs} are assumed to follow an Arrhenius dependence on temperature. These rate constants are [16,17]:

$$k_{\mathrm{d}} = k'_{\mathrm{d}}\exp\left(-\frac{E_{\mathrm{d}}}{RT}\right) \tag{18}$$

$$k_{\mathrm{p}} = k'_{\mathrm{p}}\exp\left(-\frac{E_{\mathrm{p}}}{RT}\right) \tag{19}$$

$$k_{\mathrm{to}} = k'_{\mathrm{to}}\exp\left(-\frac{E_{\mathrm{to}}}{RT}\right) \tag{20}$$

$$k_{\mathrm{f}} = k'_{\mathrm{f}}\exp\left(-\frac{E_{\mathrm{f}}}{RT}\right) \tag{21}$$

The expression for k_{t} is obtained using (20) and the Schmidt-Ray correlation for the gel effect [16–18]:

$$g_{\mathrm{t}} = \frac{k_{\mathrm{t}}}{k_{\mathrm{to}}} = \begin{cases}0.10575\exp[17.15V_{\mathrm{f}}-0.01715(T-273.2)]\\ V_{\mathrm{f}} > [0.1856-2.965\times10^{-4}(T-273.2)]\\ 2.3\times10^{-6}\exp[75V_{\mathrm{f}}]\\ V_{\mathrm{f}} \le [0.1856-2.965\times10^{-4}(T-273.2)]\end{cases} \tag{22}$$

The free volume V_{f} is calculated from the volume fractions of monomer, polymer, and solvent in the rector through the following equations [16–18]:

$$\Omega = V_{\mathrm{fm}}\phi_{\mathrm{m}}+V_{\mathrm{fp}}\phi_{\mathrm{p}}+V_{\mathrm{fs}}\phi_{\mathrm{s}} \tag{23}$$

$$V_{\mathrm{f}} = \begin{cases}\Omega & \text{if } \Omega > 0\\ 0 & \text{if } \Omega \le 0\end{cases} \tag{24}$$

where

$$V_{\mathrm{fm}} = 0.025+0.001(T-167) \tag{25}$$

$$V_{\mathrm{fp}} = 0.025+0.00048(T-378) \tag{26}$$

$$V_{\mathrm{fs}} = 0.025+0.001(T-181) \tag{27}$$

Volume fractions are calculated using the reactor concentrations and physical property data under the assumption of ideal mixing [17]

$$\phi_{\mathrm{m}} = \frac{\mathrm{MW_m}M}{\rho_{\mathrm{m}}} \tag{28}$$

$$\phi_{\mathrm{i}} = \frac{\mathrm{MW_i}M}{\rho_{\mathrm{i}}} \tag{29}$$

$$\phi_{\mathrm{s}} = \frac{\mathrm{MW_s}M}{\rho_{\mathrm{s}}} \tag{30}$$

$$\phi_{\mathrm{p}} = \frac{\rho - \phi_{\mathrm{m}}\rho_{\mathrm{m}} - \phi_{\mathrm{s}}\rho_{\mathrm{s}} - \phi_{\mathrm{i}}\rho_{\mathrm{i}}}{\rho_{\mathrm{p}}} \tag{31}$$

where MW_j is the molecular weight of species j, ρ_j is the pure component density of species j, and ρ is the density of the fluid in the reactor (which is assumed to be constant). The equation for ϕ_{p} is derived from the requirement that the mass fractions in the reactor sum to unity. The initiator concentration in the reactor usually is very low relative to the other species. As a result, it is reasonable to make the approximation $\phi_i = 0$ [17].

The polymerization reactor equations are nondimensionalized using the dimensionless variables, as shown in Table 1, to give the following state-space model [16]:

$$\frac{dx_1}{d\tau} = x_{1\mathrm{f}} - x_1 - Da_{\mathrm{p}}Wx_1E_{\mathrm{x}} \tag{32}$$

$$\frac{dx_2}{d\tau} = -x_2 - BDa_{\mathrm{p}}\gamma_{\mathrm{p}}Wx_1E_{\mathrm{x}} - \beta(x_2 - x_{2\mathrm{c}}) \tag{33}$$

$$\frac{dx_3}{d\tau} = x_{3\mathrm{f}} - x_3 - Da_{\mathrm{d}}x_3E_{\mathrm{xd}} \tag{34}$$

$$\frac{dx_4}{d\tau} = x_{4\mathrm{f}} - x_4 \tag{35}$$

$$\frac{dx_5}{d\tau} = -x_5 + [(Da_{\mathrm{f}}x_1E_{\mathrm{xf}} + Da_{\mathrm{s}}x_4 + g_{\mathrm{t}}Da_{\mathrm{td}}WE_{\mathrm{xtd}})(\alpha W)] + \frac{1}{2}W^2g_{\mathrm{t}}Da_{\mathrm{tc}}E_{\mathrm{xtc}} \tag{36}$$

$$\frac{dx_6}{d\tau} = -x_6 + [(Da_{\mathrm{f}}x_1E_{\mathrm{xf}} + Da_{\mathrm{s}}x_4 + g_{\mathrm{t}}Da_{\mathrm{td}}\mathrm{WE_{xtd}})(2\alpha - \alpha^2) + g_{\mathrm{t}}Da_{\mathrm{tc}}\mathrm{WE_{xtc}}] + W(1-\alpha) \tag{37}$$

Table 1
Dimensionless variables [16]

Dimensionless variable	Definition	Dimensionless variable	Definition
τ	$\frac{tq}{V}$	γ_{p}	$\frac{E_{\mathrm{p}}}{RT_{\mathrm{f}}}$
x_1	$\frac{M}{M_{\mathrm{fo}}}$	γ_{t}	$\frac{E_{\mathrm{t}}}{E_{\mathrm{p}}}$
x_2	$\frac{T-T_{\mathrm{f}}}{T_{\mathrm{f}}}\,\frac{E_{\mathrm{p}}}{RT_{\mathrm{f}}}$	γ_{d}	$\frac{E_{\mathrm{d}}}{E_{\mathrm{p}}}$
x_3	$\frac{I}{M_{\mathrm{fo}}}$	γ_{tc}	$\frac{E_{\mathrm{tc}}}{E_{\mathrm{p}}}$
x_4	$\frac{S}{M_{\mathrm{fo}}}$	γ_{td}	$\frac{E_{\mathrm{td}}}{E_{\mathrm{p}}}$
x_5	$\frac{\lambda}{M_{\mathrm{fo}}}$	γ_{f}	$\frac{E_{\mathrm{f}}}{E_{\mathrm{p}}}$
x_6	$\frac{\lambda_1}{M_{\mathrm{fo}}}$	η	$\frac{k'_{\mathrm{d}}\,e^{-\gamma_{\mathrm{d}}\gamma_{\mathrm{p}}}}{k'_{\mathrm{p}}M_{\mathrm{fo}}\,e^{-\gamma_{\mathrm{p}}}}$
x_7	$\frac{\lambda_2}{M_{\mathrm{fo}}}$	Da_{p}	$\frac{k'_{\mathrm{p}}\,e^{-\gamma_{\mathrm{p}}}\,VM_{\mathrm{fo}}}{q}$
W	$\frac{P}{M_{\mathrm{fo}}}$	Da_{d}	ηDa_{p}
$x_{1\mathrm{f}}$	$\frac{M_{\mathrm{f}}}{M_{\mathrm{fo}}}$	Da_{s}	$\frac{k_{\mathrm{fs}}M_{\mathrm{fo}}V}{q}$
$x_{2\mathrm{c}}$	$\frac{T_{\mathrm{c}}-T_{\mathrm{f}}}{T_{\mathrm{f}}}\,\frac{E_{\mathrm{p}}}{RT_{\mathrm{f}}}$	Da_{t}	$\frac{k'_{\mathrm{to}}\,e^{-\gamma_{\mathrm{t}}\gamma_{\mathrm{p}}}\,VM_{\mathrm{fo}}}{q}$
$x_{3\mathrm{f}}$	$\frac{I_{\mathrm{f}}}{M_{\mathrm{fo}}}$	Da_{tc}	$\frac{k'_{\mathrm{tco}}\,e^{-\gamma_{\mathrm{to}}\gamma_{\mathrm{p}}}\,VM_{\mathrm{fo}}}{q}$
B	$\frac{(-\Delta H)M_{\mathrm{fo}}}{\rho c_{\mathrm{p}}T_{\mathrm{f}}}$	Da_{td}	$\frac{k'_{\mathrm{tdo}}\,e^{-\gamma_{\mathrm{td}}\gamma_{\mathrm{p}}}\,VM_{\mathrm{fo}}}{q}$
β	$\frac{hA_{\mathrm{c}}}{\rho c_{\mathrm{p}}q}$	Da_{f}	$\frac{k'_{\mathrm{f}}\,e^{-\gamma_{\mathrm{f}}\gamma_{\mathrm{p}}}\,VM_{\mathrm{fo}}}{q}$

$$\frac{dx_7}{d\tau} = -x_7 + [(Da_{\mathrm{f}}x_1E_{\mathrm{xf}} + Da_{\mathrm{s}}x_4 + g_{\mathrm{t}}Da_{\mathrm{td}}\mathrm{WE_{xtd}})(\alpha^3 - 3\alpha^2 - 4\alpha) + g_{\mathrm{t}}Da_{\mathrm{tc}}\mathrm{WE_{xtc}}(\alpha + 2)] + W(1-\alpha)^2 \tag{38}$$

where

$$\alpha = \frac{Da_{\mathrm{p}}x_1E_{\mathrm{x}}}{Da_{\mathrm{p}}E_{\mathrm{x}}x_1 + Da_{\mathrm{f}}E_{\mathrm{xf}}x_1 + g_{\mathrm{t}}Da_{\mathrm{t}}\mathrm{WE_{xt}} + Da_{\mathrm{s}}x_4} \tag{39}$$

$$E_{\mathrm{x}} = \exp\left[\frac{x_2}{1 + (x_2/\gamma_{\mathrm{p}})}\right] \tag{40}$$

$$E_{\mathrm{xj}}\ \exp\left[\frac{\gamma_j x_2}{1 + (x_2/\gamma_{\mathrm{p}})}\right], \quad (j \equiv d, f, t, \mathrm{tc}, \mathrm{td}) \tag{41}$$

The parameter values of model equations are given in Table 2.

3.1.1. Open-loop results

The open-loop behavior of the system has been justified using simulations on steady-state responses. Moreover, using the transient responses of the state variables, may give a better understanding of the open-loop dynamics, i.e., monomer and initiator concentration in the reactor, rector temperature, and three leading moments.

The feed conditions for a start up and initial values are summarized in Table 3. The start up procedure is as follows:

For $t < 0$, the reactor contains only the monomer and solvent which are at a same temperature with that of the cooling jacket and feed. At this time, in order to reach the desired conversion, the concentration of the monomer feed and the reactor monomer is kept at the same level.

It is assumed that no reaction takes place before the feed enters the reactor. At time zero, monomer, initiator, and solvent are applied to the reactor. Immediately, the reaction starts until the system reaches its steady state. The open-loop steady-state results are listed in Table 4 as the main case of simulation.

The open-loop responses, for start up of the CSTR system, are illustrated in Fig. 4. It is observed that the monomer concentration in the reactor, changes from 3.5 mol/L to a new steady-state value as 3.14 mol/L. This is due to both the monomer consumption and increase in the moments from zero to their steady-state values. Moreover, the reactor temperature rises rapidly, mainly because of the exothermic nature of the reaction.

3.1.2. Step response results

In the polymerization process, the MWD is largely determined by the first three moments of the distribution which are often called the principle moment. In this application, the principle moments are unique function of the reactor state variables x_1–x_4 at steady state [17]. Moreover, it has been proved that the steady-state values of initiator and solvent concentration are depended on model parameters such as feed condition and the reactor temperature [17]. Thus, by driving the monomer concentration (x_1) and the reactor temperature (x_2) to particular set points, the MWD can be controlled approximately. This implies that polymer grades corresponding to different steady-state conditions and the same feed conditions can be obtained using the controlled variables and the monomer feed concentration and the coolant temperature as manipulated variables.

In order to obtain settling and sampling time of the process, some step tests are performed. Suppose that T_{st} be the process settling time, then the sampling time can be chosen in range of $T_{\mathrm{st}}/100$ to $T_{\mathrm{st}}/20$ [5]. Moreover, this test is helpful for studying the nonlinear behavior of the process. The step tests are performed by changing each of the two manipulated variables independently of the other manipulated variable. Fig. 5 shows the open-loop responses

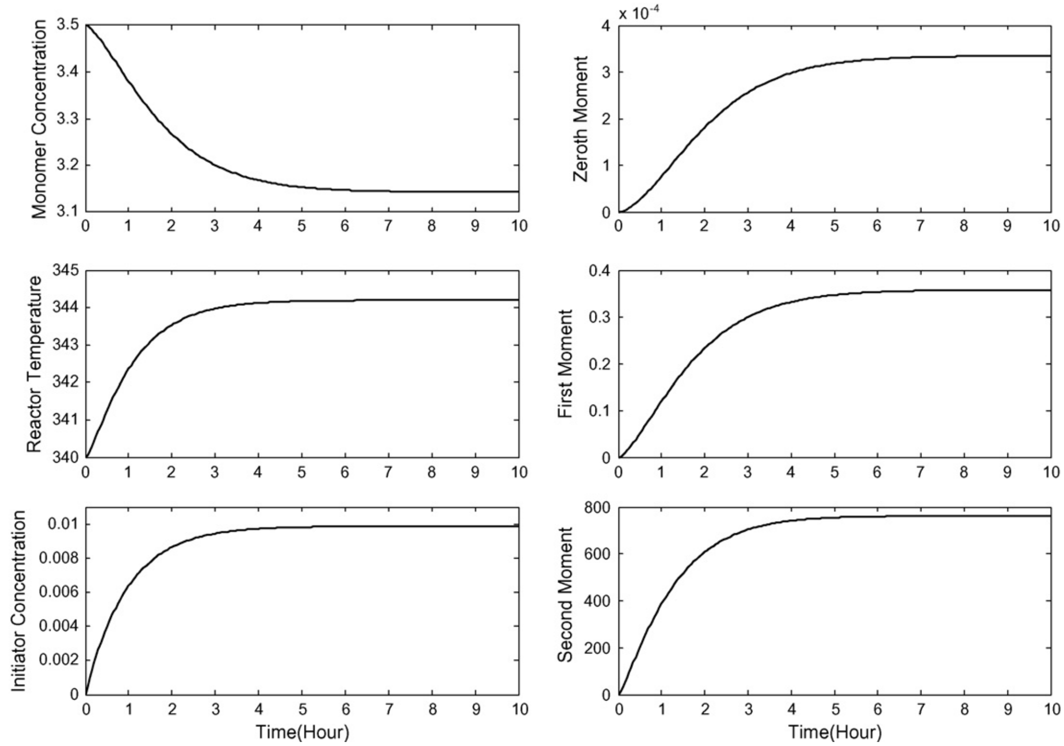

Fig. 4. Open-loop response of polymerization process.

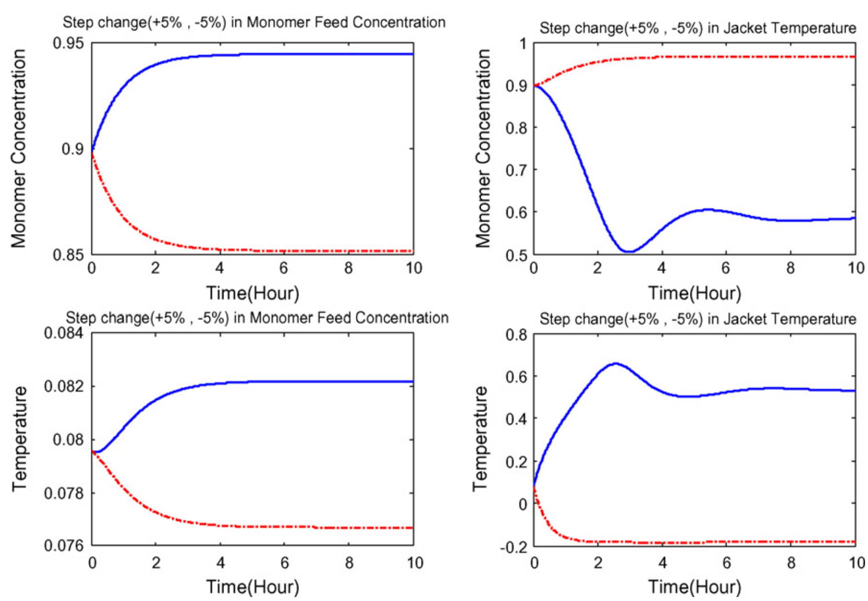

Fig. 5. The open-loop responses for ±5% step changes (+5% solid line, −5% dashed line) in manipulated variables.

Table 2
parameters and constant values in polymerization reactor model [18]

Variable	Value	Variable	Value	Variable	Value
ρ	1038 g/L	k'_d	1.69×10^{14} S^{-1}	E_d	3000 cal/mol
ρ_s	898.5 g/L	k'_p	4.925×10^5 L/mol s	E_p	4353 cal/mol
ρ_i	1000 g/L	k'_{to}	9.80×10^7 L/mol s	E_{to}	701 cal/mol
ρ_m	942.11 g/L	k'_f	4.92 L/mol s	E_f	4353 cal/mol
ρ_p	1200 g/L	k'_{fs}	0.091	f	0.5
c_p	0.4 cal/(g K)	$\frac{k_{td}}{k_{tc}}$	8.23	h	135.6 mol/(m^2 s K)
V	900 L	A_c	2.8 m^2	$-\Delta H$	13.8 kcal/mol
q	0.2813 L/s	MW_m	100.13 g/mol	MW_s	88.12 g/mol
R	0.001987	MW_i	24.23 g/mol	M_{fo}	3.5 g mol/L

Table 3
Feed condition for startup [18]

Monomer feed concentration (M_f)	3.5 gmol/L
Initiator feed concentration (I_f)	0.01 gmol/L
Solvent feed concentration (S_f)	6.4 gmol/L
Feed temperature (T_f)	340 K
Feed temperature (T_c)	340 K
Total feed flow rate	1800 L/h

Table 4
Base case for simulation [18]

Monomer concentration	3.146 gmol/L
Initiator concentration	0.0097 gmol/L
Solvent concentration	6.4 gmol/L
Zeroth moment	3.3×10^{-4}
First moment	0.35
Second moment	759.53
Reactor temperature	344.2 K
Number average chain length	1076.14
Polydispersity	1.9937

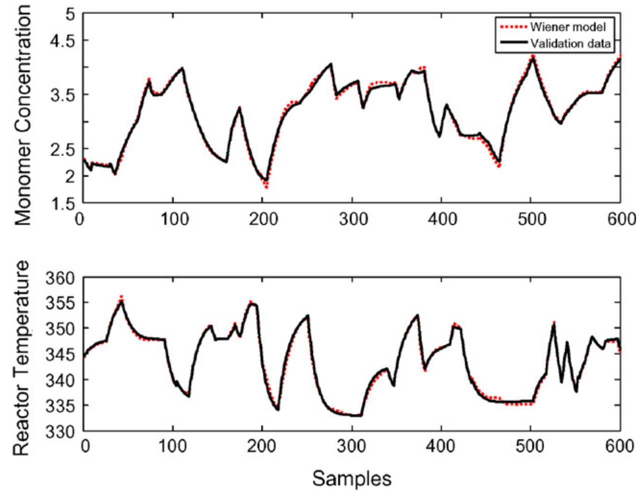

Fig. 7. Validation of the Wiener model for polymerization process.

for ±5% step changes in manipulated variables. It can be seen that the polymerization process has severe nonlinearity for step changes at coolant temperature.

3.2. Identification of the process

A GMN signal is used as a random sequence input in order to obtain dynamic data. In this test, seven levels 2, 2.5, 3, 3.5, 4, 4.5 and 5 have been selected for the first input (monomer feed concentration) and seven levels 326, 330, 335, 340, 345, 350 and 353 for the second input (jacket temperature) to cover the spanned range of the input signal. Switching time between these levels is assumed to be 15 samples. Both two signals obtained from GMN test are applied to the process simultaneously. Two thousand samples of the input–output data with sampling time of 180 s are used for identification. The input and output signals of polymerization process are shown in Fig. 6.

The model parameters for the linear block were computed using a state-space description and input/output dynamic data. A steady-state data set has been used in the identification of the Wiener static gain. 400 steady-state data for linear model and 400 steady-state data for process have been obtained. The static nonlinear gain is approximated using these steady-state data and piecewise linear functions.

Finally, the Wiener model is identified by the linear model outputs and process nonlinear gain. From the 2000 obtained data, 1400 samples are used for identification and the rest is used for validation. Fig. 7 shows that the identified Wiener model is in good agreement with process behavior.

3.3. Nonlinear model predictive control

In this section, the nonlinear model predictive control based on the piecewise linear Wiener model is applied to polymeriza-

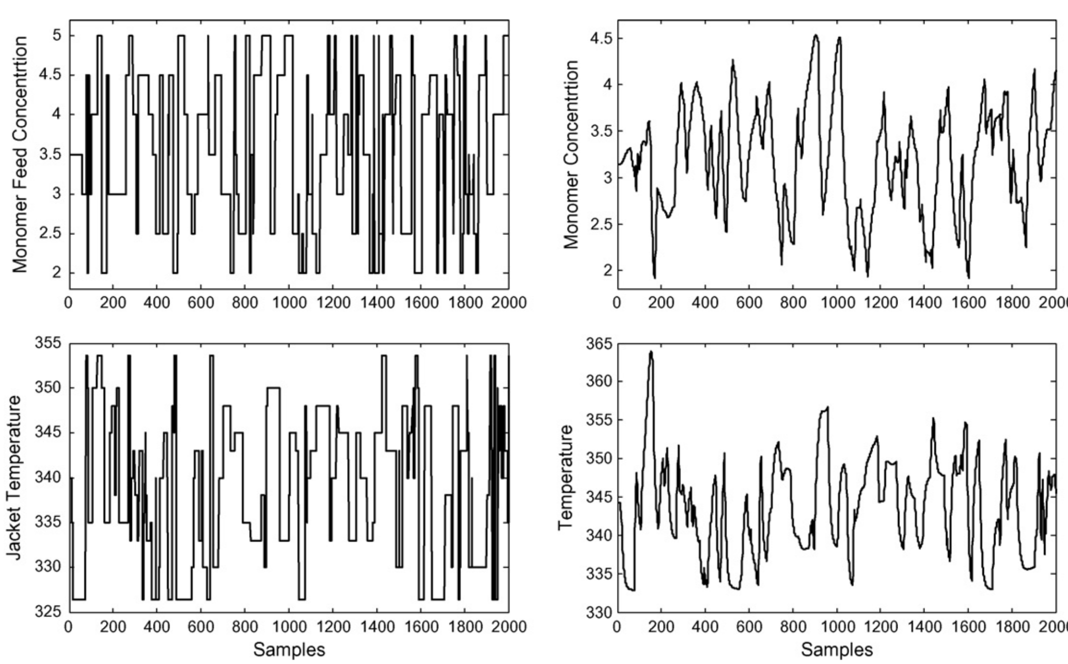

Fig. 6. GMN inputs (monomer feed concentration and jacket temperature) and output signals (monomer concentration and reactor temperature) for identification of polymerization reactor.

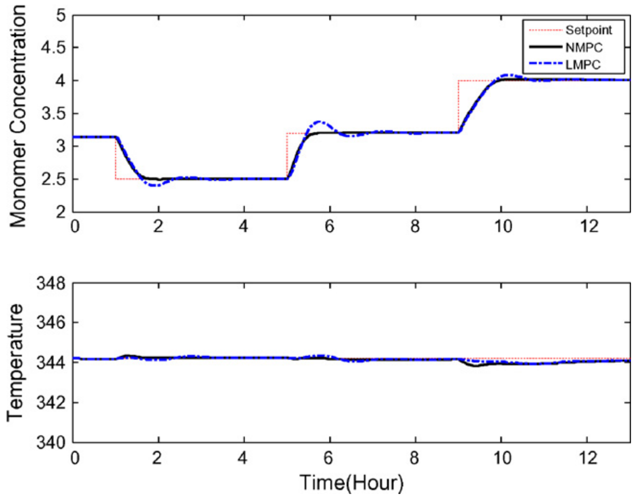

Fig. 8. Comparison the behavior of NMPC (solid line) and linear MPC (dashed line) for set point changes in monomer concentration output.

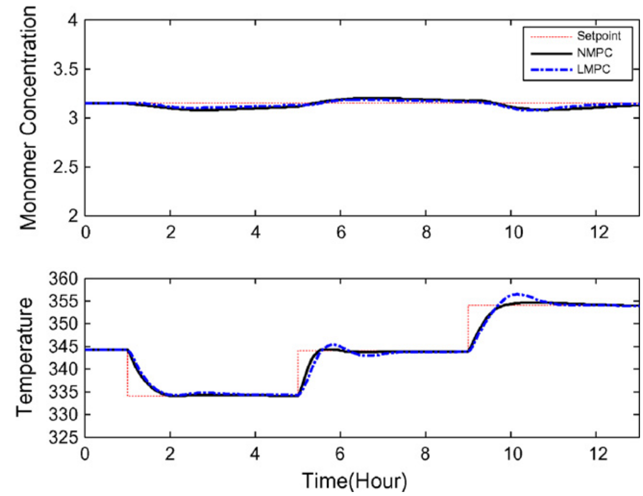

Fig. 10. Comparison the behavior of NMPC (solid line) and LMPC (dashed line) for set point changes in reactor temperature.

tion reactor. This process is a multi-input multi-output process and NMPC of this process is done with concentration on practical aspects such as excitation signal for identification and rejection of disturbance effects in this process.

The parameters for the NMPC are defined as follows: the control and prediction horizons are tuned 3 and 10, respectively. The weighting matrix **Q** takes the value 100 for both process outputs, **R** takes the value 50 for monomer feed concentration and 100 for coolant temperature. It is noticeable that the weighting matrices are determined by trial and error as well as prediction and control horizons.

The simulation results for this control scheme have been compared to LMPC. Parameters of both linear and nonlinear controllers are tuned and the best obtained results are compared. For both cases (NMPC and linear MPC) a range of 2–5 for monomer feed concentration input and a range of 326–353 for coolant temperature input has been considered as input constraints.

Fig. 8 shows a comparison of NMPC and LMPC behavior for polymerization process when the first output set points have changed, where the second output is set to the nominal value, 344.2. Control signals of both controllers are shown in Fig. 9. As it is clear from these figures the NMPC controller has better performance with short settling time and without any overshoot. Furthermore, the second output has been maintained closed to the nominal value. Control signals of both controllers do not have any large step changes.

A comparison of NMPC and LMPC behavior for set point change in reactor temperature has been shown in Fig. 10, where the first output (monomer concentration) is set to the nominal value, 3.15. Fig. 11 shows a comparison of corresponding control signals. Results show that nonlinear controller has a better performance compared to the linear one regarding set point changes in reactor temperature.

In Fig. 12, the NMPC performance for set points changes in both outputs has been compared to LMPC. It can be seen that the nonlinear controller has a much better performance compared to the linear one; it has a short settling time without overshoot. The comparison of corresponding control signals of both controllers are presented in Fig. 13. It is shown that the control signals of both controllers are almost smooth. Moreover, the defined constraints for

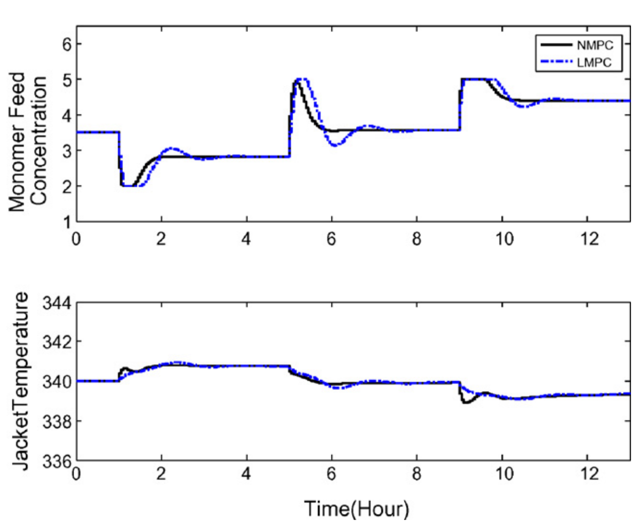

Fig. 9. Comparison control signal of NMPC (solid line) with linear MPC (dashed line) for set point changes in monomer concentration output.

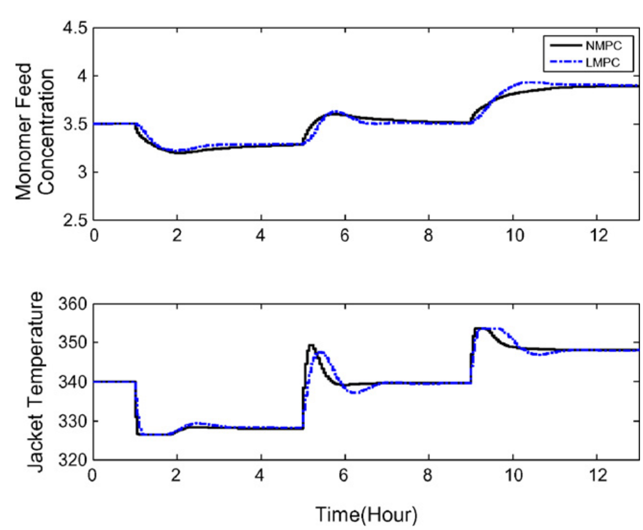

Fig. 11. Comparison control signal of NMPC (solid line) with linear MPC (dashed line) for set point changes in reactor temperature output.

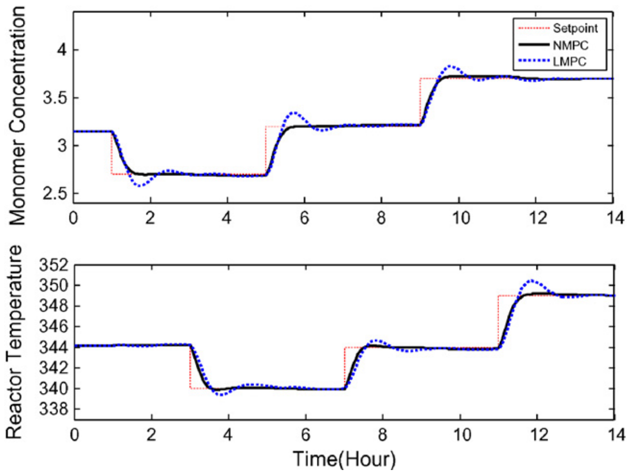

Fig. 12. Comparison the NMPC (solid line) and LMPC (dashed line) performance for set point changes in both process outputs.

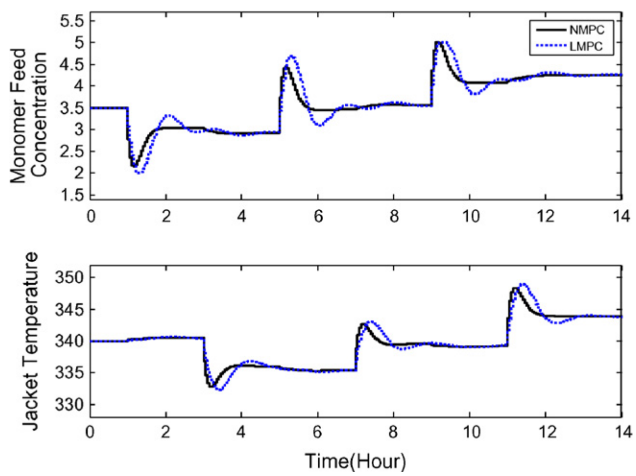

Fig. 13. Comparison control signal of NMPC (solid line) and LMPC (dashed line) for set point changes in both process outputs.

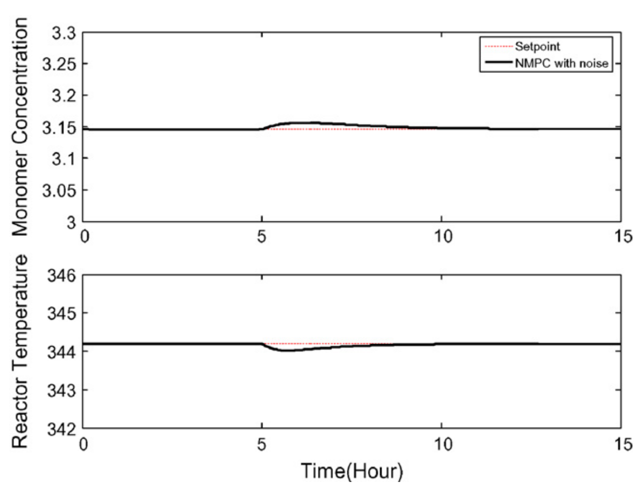

Fig. 14. The NMPC performance in rejecting unmeasured disturbance of the initiator efficiency factor, *f*.

manipulated variables are satisfied. All of the simulations showed that the maximum computation time for optimization at each sampling interval is sufficiently below the chosen sampling time and the control signals are feasible due to canonical structure of nonlinear gain.

The NMPC performance in rejecting unmeasured disturbance of initiator efficiency factor, f is shown in Fig. 14. Here, the initiator efficiency factor, f decreases from 0.5 to 0.45. It can be seen that NMPC is able to reject unmeasured disturbance effectively.

4. Conclusions

In this paper, a nonlinear model predictive control based on a piecewise linear Wiener model for a polymerization reactor is applied and simulated. This approach has all the interesting features of classical MPC. It leads to a quadratic programming problem due to the canonical structure of the nonlinear gain, so it has easy computations. On the other hand, the identification of the nonlinear gain of the process using piecewise linear approximation needs both dynamic and steady-state input–output data. This method can be implemented on multivariable and highly nonlinear processes which LMPC is unable to control them. The presented control scheme is applied to a polymerization reactor as a MIMO process. Simulation results show superior performance of the NMPC compare to LMPC. Results show that the linear MPC follows the set point with overshoot and long settling time, while the NMPC exhibits a desirable fast response with smooth changes in the control effort. Furthermore, it rejects unmeasured disturbance effectively.

References

[1] S.J. Qin, T.A. Badgwell, An overview of nonlinear model predictive applications, in: IFAC Workshop on Nonlinear Model Predictive Control, Assessment and Future Direction, Ascona, Switzerland, 1998.
[2] S.J. Qin, T.A. Badgwell, A survey of model predictive control technology, Control Eng. Pract. 11 (2003) 733–764.
[3] E.F. Camacho, C. Bordons, Model Predictive Control, 2nd ed., Springer-Verlag, London, 2004.
[4] M.A. Henson, Nonlinear model predictive control: current status and future directions, Comput. Chem. Eng. 23 (1998) 187–202.
[5] Y. Zhu, Multivariable System Identification for Process Control, Pergamon, an imprint of Elsevier Science, 2001.
[6] A. Janczak, Identification of Nonlinear Systems Using Neural Networks and Polynomial Models: A Block-Oriented Approach, Springer-Verlag, Berlin, Heidelberg, 2005.
[7] A.L. Cervantes, O.E. Agamennoni, J.L. Figueroa, A nonlinear model predictive control system based on Wiener piecewise linear models, J. Process Contr. 13 (2003) 655–666.
[8] J.C. Gomez, A. Jutan, E. Baeyens, Wiener model identification and predictive control of a pH neutralization process, IEE Proc. Control Theory Appl. 151 (3) (2004) 329–338.
[9] S.J. Norquay, A. Palazoglu, J.A. Romagnoli, Model predictive control based on Wiener models, Chem. Eng. Sci. 53 (1) (1998) 75–84.
[10] A.L. Cervantes, O.E. Agamennoni, J.L. Figueroa, Use of Wiener nonlinear MPC to control a CSTR with multiple steady state, Latin Am. Appl. Res. 33 (2003) 149–154.
[11] G. Shafiee, M.M. Arefi, M.R. Jahed-Motlagh, A.A. Jalali, Model Predictive control of a highly nonlinear process based on piecewise linear Wiener models, in: 1st IEEE int. Conf. E-Learning in Indust. Elec., 2006, pp. 113–118.
[12] G.B. Sentoni, L.T. Biegler, J.B. Guiver, H. Zhao, State-space nonlinear process modeling: identification and universality, AIChE J. 44 (10) (1998) 2229–2239.
[13] M.M. Arefi, A. Montazeri, M.R. Jahed-Motlagh, J. Poshtan, Nonlinear model predictive control of chemical processed with a Wiener identification approach, in: IEEE Int. Conf. Indust. Tech., 2006, pp. 1735–1740.
[14] M.M. Arefi, A. Montazeri, J. Poshtan, M.R. Jahed-Motlagh, Wiener-neural identification and predictive control of a more realistic plug-flow tubular reactor, Chem. Eng. J. 138 (1–3) (2008) 274–282.
[15] H.H.J. Bloemen, C.T. Chou, T.J.J. van den Boom, V. Verdult, M. Verhaegen, T.C. Backx, Wiener model identification and predictive control for dual composition control of a distillation column, J. Process Contr. 11 (6) (2001) 601–620.
[16] A.K. Adebekun, F.J. Schork, Continuous solution polymerization reactor control. Part 2. Estimation and nonlinear reference control during methyl methacrylate polymerization, Ind. Eng. Chem. Res. 28 (1989) 1846–1861.

[17] M.J. Kurtz, G.Y. Zhu, M.A. Henson, Constrained output feedback control of a multivariable polymerization reactor, IEEE T. Contr. Syst. T. 8 (1) (2000) 87–97.
[18] Z. Liu, CMPC control of solution polymerization of methyl methacrylate in CSTR, PHD Thesis, Department of chemical Engineering, University of Louisville, Louisville, Kentucky, USA, December 1997.
[19] B.G. Jeong, K.Y. Yoo, H.K. Rhee, Nonlinear model predictive control using a Wiener model of a continuous Methyl Methacrylate Polymerization reactor, Ind. Eng. Chem. Res. 40 (25) (2001) 5968–5977.
[20] H.J. Rho, Y.J. Huh, H.K. Rhee, Application of adaptive model-predictive control to a batch MMA polymerization reactor, Chem. Eng. Sci. 53 (21) (1998) 3729–3739.
[21] L. Ozkan, M.V. Kothare, C. Georgakis, Control of a solution copolymerization reactor using multi-model predictive control, Chem. Eng. Sci. 58 (2003) 1207–1221.
[22] D. Westwick, M. Verhaegen, Identifying MIMO Wiener system using subspace model identification methods, Signal Process. 52 (2) (1996) 235–258.
[23] P. Julian, A. Desages, O. Agamennoni, High level canonical piecewise linear representation using a simplicial partition, IEEE T. Circuits-I 46 (1999) 463–480.
[24] P. Julian, High level canonical piecewise linear representation: theory and applications, PHD Thesis, DIEC-Universidad Nacional del Sur, Bahıa Blanca, Buenos Aires, Argentina, 1999.
[25] R.K. Pearson, M. Pottmann, Gray-box identification of block-oriented nonlinear models, J. Process Contr. 10 (2000) 301–315.
[26] S. Gerksic, D. Juricic, S. Strmcnik, M. Matko, Wiener model based nonlinear predictive control, Int. J. Syst. Sci. 31 (2000) 189–202.
[27] P. Julian, A Toolbox for the Piecewise Linear Approximation of Multidimensional Functions, available from: http://www.pedrojulian.com, 2000.
[28] J.L. Figueroa, A. Desages, Use of piecewise linear approximations for steady-state back-off analysis, Optim. Contr. Appl. Met. 19 (1998) 93–110.